T7 RNA Polymerase Studied by Force Measurements Varying Cofactor Concentration

P. Thomen,* P. J. Lopez,† U. Bockelmann,‡ J. Guillerez,§ M. Dreyfus,§ and F. Heslot*

*École Normale Supérieure, Laboratoire Pierre Aigrain, CNRS UMR 8551, Université Pierre et Marie Curie, Paris, France; †École Normale Supérieure, Laboratoire de Biominéralisation et Morphogenèse des Diatomées, CNRS UMR 8183, Paris, France; ‡Laboratoire de Nanobiophysique, École Supérieure de Physique et Chimie Industrielles, Paris, France; and §École Normale Supérieure, Laboratoire de Génétique Moléculaire, Paris, France

ABSTRACT RNA polymerases carry out the synthesis of an RNA copy from a DNA template. They move along DNA, incorporate nucleotide triphosphate (NTP) at the end of the growing RNA chain, and consume chemical energy. In a single-molecule assay using the T7 RNA polymerase, we study how a mechanical force opposing the forward motion of the enzyme along DNA affects the translocation rate. We also study the influence of nucleotide and magnesium concentration on this process. The experiment shows that the opposing mechanical force is a competitive inhibitor of nucleotide binding. Also, the single-molecule data suggest that magnesium ions are involved in a step that does not depend on the external load force. These kinetic results associated with known biochemical and mutagenic data, along with the static information obtained from crystallographic structures, shape a very coherent view of the catalytic cycle of the enzyme: translocation does not take place upon NTP binding nor upon NTP cleavage, but rather occurs after PPi release and before the next nucleotide binding event. Furthermore, the energetic bias associated with the forward motion of the enzyme is close to kT and represents only a small fraction of the free energy of nucleotide incorporation and pyrophosphate hydrolysis.

INTRODUCTION

Proteins are involved in most biological processes, and as enzymes they play important catalytic roles. In some particularly interesting cases, the catalytic cycle of the protein may be associated with a dynamical conformational change, guided by interactions with small ligand molecules. Such changes in structure associated with the catalytic cycle are exploited by linear motor proteins to generate movement (e.g., in transcription (1)), by various rotational motor proteins to induce such processes as ion pumping through membranes, ATP synthesis, or the flagellar motion of bacteria (2). Many biological motors have been studied at the molecular level (3–13). An important goal of these measurements is to understand the mechanisms by which the movement is produced and how chemical energy is converted into mechanical work. We studied an RNA polymerase (RNAP), an enzyme that carries out an essential step in gene expression, the synthesis of an RNA copy from a DNA template. Within this class of enzymes, the T7 RNAP is a model system of choice, because it is a single-unit polymerase with known crystal structures (14,15). By studying transcription at the single-molecule level, it is possible to analyze how the transcribing enzyme is sensitive to an external mechanical load force opposing or favoring the motion of the enzyme along DNA (3,8,11,13, 16,17). By varying the load force, the nucleotide concentration, and the magnesium ion concentration, very interesting information can be obtained about the mechanism of the molecular motor.

When exerting a mechanical force on the enzyme, it is of course expected that within the cycle of the enzyme, the stage where forward motion occurs should be notably affected by force. This stems from the fact that under a force, F, the enzyme that advances by a displacement x opposite to the direction of force will do so at the expense of having to furnish a mechanical work $W = Fx$. One therefore expects that as the force is increased, the forward motion will be a progressively limiting event, i.e., the time necessary to accomplish this forward motion will become a significant or dominant portion of the time necessary to accomplish the full catalytic cycle. This point of view of course assumes that the force does not denature the enzyme and that forward motion occurs during a single stage.

By taking the enzymologist's point of view of force as a possible inhibitor of translocation, it is possible to analyze the characteristics of motors without making assumptions a priori about the detailed mechanism of translocation. Simple reaction cycles can be reduced to two steps, binding of substrate and catalysis:

$$E + S \rightleftarrows ES \rightarrow E + P,$$

where E, S, and P designate the enzyme, substrate, and product, respectively. This scheme assumes that the reaction is irreversible (as is the case, for example, when the product concentration is very small). The velocity of the reaction is given by the Michaelis-Menten expression,

$$V = \frac{V_m}{(1 + K_m/[S])},$$

Submitted November 23, 2007, and accepted for publication April 11, 2008.

Address reprint requests to Francois Heslot, École Normale Supérieure, Laboratoire Pierre Aigrain, CNRS UMR 8551, Université Pierre et Marie Curie, 24 rue Lhomond, 75005 Paris, France. E-mail: heslot@lpa.ens.fr.

Editor: Taekjip Ha.

0006-3495/08/09/2423/11 $2.00

doi: 10.1529/biophysj.107.125096

where $1/K_m$ stands for the apparent affinity constant of the enzyme for the substrate, and V_m for the maximum velocity. A convenient representation consists of using a Lineweaver-Burke (LB) representation, in which the inverse of the velocity of the reaction $1/V$ is plotted against the inverse of the nucleotide concentration 1/[NTP], at different levels of force. In such an LB plot, ($1/V$ vs. $1/[S]$), a linear dependence is obtained for the above reaction scheme. The slope of the corresponding line is K_m/V_m, and the intercept on the y axis (i.e., at $1/[S] = 0$), is $1/V_m$.

Three modes of action of an inhibitor (I) on the above reaction cycle can be distinguished. 1), A competitive inhibitor I interacts with E to form an ''EI complex'' in competition with S. In this case, a load force can be considered as an inhibitor opposing the binding of the substrate to the enzyme. 2), An uncompetitive inhibitor interacts with the ES complex to form ESI and prevents catalysis. 3), A noncompetitive inhibitor interacts with both E and ES to form EI or ESI. In the latter case, the effect of the inhibitor on the enzyme, E, can be different from its effect on the complex ES, leading to partially noncompetitive inhibition (see Table 1). The LB plot is a simple way to distinguish between these cases, since the Michaelis-Menten expression still holds but the constants V_m and/or K_m are modified. Table 1 gives the characteristics of each case, along with the LB graphical signature, and the corresponding interpretation in terms of K_m and V_m.

A commonly used reaction scheme for transcription is

$$E + NTP \overset{K_{Diss}}{\rightleftarrows} E - NTP \rightleftarrows \ldots\ldots \rightarrow E + PPi,$$

where E, NTP, and PPi stand for the polymerase, nucleotide triphosphate (NTP), and pyrophosphate, respectively. As mentioned before, a load force is expected to act in particular on the step coupled to forward motion. In our study on the T7 RNAP, we measured the mean elongation velocity at different load forces and different nucleotide concentrations. In a previous publication (18), we showed that for a given force, varying the nucleotide concentration, the experimental data is fitted by a straight line in an LB plot. Furthermore, when the force is varied, the slopes of the corresponding lines vary, with the important feature that the lines obtained at different forces intercept a common point on the y axis. This suggests that force acts as a competitive inhibitor of translocation.

In this article, we describe the experimental setup and the preparation of molecular constructions (Materials and Methods); we interpret the data on the influence of force on velocity with respect to the commonly invoked models (Brownian ratchet and power stroke) and present data on the combined effect of nucleotide and magnesium concentration.

MATERIALS AND METHODS

DNA construction

We have chosen a configuration in which the enzyme is specifically attached to a glass slide (Fig. 1). The template to be transcribed is the lambda DNA (~48,500 basepairs), but modified at both extremities: one extremity is labeled with a digoxygenin group (to bind to a bead covered with antibodies directed against digoxygenin), and the other contains a T7 promoter. To prepare this molecular construction, first a 10:1 molar excess (with respect to lambda DNA) of a pair of oligonucleotides that incorporates a sequence with a T7 promoter and a 5′ cohesive overhang is annealed and ligated to one of the cohesive extremities of lambda DNA. Then a 100:1 molar excess of an oligonucleotide with a digoxygenin group is annealed and ligated to the other cohesive extremity of lambda DNA. The DNA corresponding to the construction is then purified using membrane ultrafiltration; this step eliminates the excess of oligonucleotides. The sequence after the promoter is designed to have only three kinds of bases (G, A, and C) for the first 15 bases to be transcribed, the sixteenth base being T. The T7 gene 10 promoter (−17 to +13) is used:

$$\begin{array}{c} 5'\ \text{taatacgactcactatagggagaccacaacggt}\ 3'. \\ -17 \qquad\qquad +1 \end{array}$$

Initially, only GTP, ATP, and CTP nucleotides are introduced, leading to a complex stalled at +16. The complex stalled on DNA is then purified. Just before the force measurement, the four nucleotides (GTP, ATP, CTP, and UTP) are added to resume transcription.

The polymerase-DNA complex has to be stable long enough to allow for the sample preparation before adding the fourth NTP. In contrast with the *E. coli* RNAP, the T7-RNAP-DNA initiation complex is poorly stable. However the elongation complex (EC), resulting from a conformational change after the transcription of ~10–15 nucleotides (19,20), is known to be more stable than the initiation complex (IC, the first stage of transcription), the typical dissociation time of the EC being of the order of tens of minutes. The complex stalled on DNA is then quickly purified (see below). The transcribed segment upstream of the stall site is assumed to be short enough to avoid the binding of more than one enzyme on the template. The low affinity of the polymerase for the promoter forced us to use high nucleotide and enzyme concentrations in the initiation steps. This meant purifying the initial mix (containing the stalled complexes) to eliminate the free nucleotides and the free enzymes. The method we used is based on centrifugation in a sucrose gradient, and is described briefly below.

The initiation mixture (5 μl) is prepared in initiation buffer (40 mM Tris-acetate, pH 7.9, 8 mM magnesium acetate, 1 mM dithiothreitol, 0.1 mM EDTA), containing ~1 nM DNA, nucleotides (0.4 mM each, except UTP), and ~100 nM biotin-labeled T7 RNAP (see later); ~10^5 beads (covered with antibodies directed against digoxygenin, for binding to one extremity of the DNA substrate) are added and allowed to bind for 1 min. This mixture is then

TABLE 1 Different types of inhibition

Competitive inhibition	Uncompetitive inhibition	Purely noncompetitive inhibition	Partially noncompetitive inhibition
		$E + I \leftrightarrow EI$ (K_i)	$E + I \leftrightarrow EI$ (K_i)
$E + I \leftrightarrow EI$	$ES + I \leftrightarrow ESI$	$ES + ESI \leftrightarrow ESI$ (K_i)	$ES + ESI \leftrightarrow ESI$ (K_i')
Lines intercept on the y axis	Lines are parallel	Lines intercept on the x axis	Lines intercept at $1/V < (>) 0$ if $K_i > (<) K_i'$
V_m is constant	K_m/V_m is constant	V_m decreases when I increases	V_m decreases when I increases
K_m increases with I	V_m and K_m decrease when I increases	K_m is constant	K_m/V_m increases with I

For each case, the possible reactions of the inhibitor I is described. E, enzyme; S, substrate, K_i and K_i' designate the affinity constant of the inhibitor, I, for E and ES, respectively). The features of the corresponding Lineweaver-Burke plot are indicated, along with the interpretation in terms of K_m and V_m.

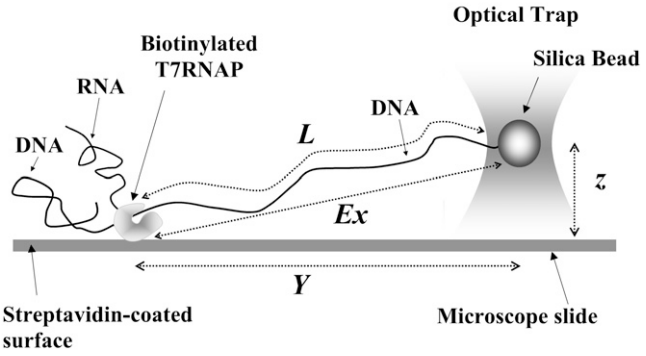

FIGURE 1 Experimental configuration. L, DNA length (L = number of bases $\times$ 0.34 nm); Ex, distance between the bead and the polymerase; z, distance between the surface and the trap; Y, distance between the polymerase and the bead, in the plane of the sample. Y and z are measured and Ex is deduced by $Ex = (Y^2 + z^2)^{1/2} - d$, where d is the radius of the bead.

centrifuged over a discontinuous sucrose gradient (five layers from 1% to 7% sucrose in initiation buffer) contained in a small tube ~15 mm in height with an internal diameter of ~4 mm. The tube is centrifuged (at ~2000 rpm) using a centrifuge with a swinging bucket rotor. During centrifugation, the beads (1 μm in diameter) that have a DNA (16 μm long) attached to them are subjected to a higher hydrodynamic friction compared to beads with no DNA attached to them. In the sucrose gradient above, it is possible in a relatively short time (1–2 min) to extract the polymerase-DNA-bead (and DNA-bead) complexes from an intermediate fraction, whereas the other species are at the bottom (beads with no DNA) or in the supernatant (free polymerases, polymerase-DNA complexes). Also, the NTPs added during the initiation stage are discarded by this centrifugation. The fraction containing polymerase-bead-DNA complexes (but no NTPs) is then supplemented with initiation buffer containing potassium glutamate (so that a final concentration of 25 mM potassium glutamate is obtained and the final volume is 100 μl) and deposited in a small well. This well is composed of a 24 $\times$ 24 mm^2 glass coverslip, with a small plastic annulus, ~13 mm in internal diameter and 1 mm in height, glued to it, so as to define a confinement region for liquid. A small round coverslip (12 mm in diameter) is then placed on top of the deposited liquid, fitting inside the plastic annulus and freely ''floating''. The glass bottom of the well is coated with streptavidin, and hence will capture the biotin-labeled T7 polymerases stalled on one end of the lambda DNA, whereas the other end of the lambda DNA is attached to a microscopic bead. The attachments of the polymerases on the surface thus lead to tethered beads in the sample. A flow is then transiently created in the sample to detect tethered beads under the microscope (18,21). After having selected a tethered bead, all four nucleotides are added at the same concentration (henceforth noted ''[NTP]'') and mixed into the sample. For the measurements with different magnesium ion concentrations, we used a similar protocol and adjusted the magnesium ion concentration by adding magnesium acetate together with nucleotides. This allowed us to study the influence of magnesium concentration during elongation, without affecting initiation.

Polymerase preparation and purification

For the construction of the biotin-tagged T7 RNAP, a BamHI fragment from pHB161 was first cloned into pUC19, then the NcoI-XbaI region was replaced by oligonucleotides, adding the amino acid sequence MAGGLNDIFEAQKMEWRLE at the N-terminus of the protein (the underlined lysine should correspond to the biotinylated amino acid). This new plasmid, named pBio-T7-RNAP, was used to transform the *E. coli* strain AVB101 (Avidity, Aurora, CO), which already contains a plasmid with an IPTG-inducible *birA* gene. At midlog growth, 1 mM IPTG and 50 μM biotin are added to the culture, and the growth is continued for an additional 3 h. The Bio-T7-RNAP is then purified on a softLink column (Promega, Madison, WI) from total soluble proteins. After elution in 50 mM Tris-HCl, pH 7.9, 100 mM NaCl, 2 mM EDTA, 0.05% Triton X100, 5% glycerol, 20 μg/ml PMSF, and 8 mM biotin, the protein was concentrated by ultrafiltration (YM100, Amicon, Houston, TX) and then extensively dialyzed against the same buffer without biotin. Finally, the Bio-T7-RNAP was dialyzed in 20 mM phosphate buffer, pH 7.7, 1 mM EDTA, 100 mM NaCl, 1 mM dithiothreitol, and 50% glycerol and stored at –80°C.

In the transcription buffer, we used potassium glutamate (KGlu) as salt instead of NaCl, to avoid adding Cl^- ions that could decrease the enzyme activity (22). KGlu is used here to prevent the nonspecific attachment of enzymes on the surface. However, the amount of salt one can add to the buffer is limited, because part of the interactions involved in the stability of the polymerase-DNA-RNA complex are of electrostatic origin (23): a high salt concentration is expected to increase the rate of spontaneous dissociation of the DNA-RNAP complex. Consistent with this, we observed more ''breakage events'' (polymerase-surface attachment breakage, DNA-polymerase dissociation, or DNA-bead attachment breakage) at 150 mM KGlu than at 25 mM KGlu. Initiation buffer supplemented with 25 mM KGlu was subsequently used in the elongation experiments. In the experiments devoted to the study of the effects of magnesium, the concentration of magnesium acetate was varied.

Measurement of force and displacement

In the setup, described previously in detail (21), interferometry is used to measure the displacement of the bead within the optical trap. In the standard mode, the voltage corresponding to the force is measured as a function of sample displacement. We also operated the optical trap in a feedback mode, where a constant force is maintained on a single molecule: the voltage corresponding to the measured force is compared with a reference voltage. The difference is amplified, integrated, and then fed back to a piezoelectric translation stage that displaces the sample laterally while the optical trap position is kept fixed. In this mode, the translocation of the enzyme along DNA is reflected by the displacement of the sample. The time constant of the regulation electronics is ~20 ms. The objective (and then the trap) can also move (by a slow drift) about the vertical axis relative to the sample. This displacement is measured by a two-quadrant photodiode attached to the objective, and illuminated by a laser diode (power of ~1 mW) whose position is static with respect to the height of the sample. This setup allows us to measure vertical displacements of ~10 nm to monitor and take into account eventual vertical drift of the objective. The position (horizontal and vertical) and the force signals are filtered by antialiasing filters at 44 Hz and sampled using a 16-bit analog-to-digital conversion at a rate of 100 Hz, and stored onto a hard disk.

The experiments have been performed at a regulated temperature of 27°C. For this regulation, resistive heaters and platinum resistive temperature detectors have been attached to the immersion objective and the sample holder. A commercial control circuit (RHM-4000, Wavelength Electronics, Martinsried, Germany) is used to regulate the temperature within 0.1°.

Elasticity of DNA

The force exerted by the enzyme on the bead (F), the distance between the surface and the trap (z), and the distance between the polymerase and the bead (Y, in the plane of the sample glass surface) (see Fig. 1) are recorded as a function of time t. The distance Ex between the bead and the polymerase is derived from the above recorded data by $Ex = (Y^2 + z^2)^{1/2} - d$, where d is the radius of the bead. The contour length, L, of the DNA between polymerase and bead is deduced from Ex and F using the following expression of DNA elasticity (24):

$$\frac{Ex}{L} = 1 + \frac{F}{K_0} - \frac{1}{2}\left(\frac{kT}{FA}\right)^{1/2},$$

where $K_0 = 1000$ pN is a constant (experimentally determined) and $A = 50$ nm is the persistence length of double-stranded DNA (dsDNA). F/K_0 stands for the stretching of the backbone of the molecule: the distance between the bases (0.34 nm at zero force) is expected to increase slightly with force. This has potentially to be taken into account in the calculation of the length, L. However, for $F < 20$ pN, $F/K_0 \approx 0.02$, which means that the force stretches the contour length of dsDNA by $<2\%$. As F is always <20 pN in our experiments, it is thus assumed that this effect is negligible. This also means that we make the conversion between the number of nanometers per second in contour length and the number of bases per second by simply dividing the contour length by 0.34 nm/bp.

RESULTS AND DISCUSSION

In most measurements presented in this article, force is kept constant by an automated displacement of the sample (see Materials and Methods), whereas the length $Ex(t)$ and $L(t)$ decrease during transcription. The analytic relation between F, Ex, and L allows us to calculate $L(t)$ from F and $Ex(t)$. The velocity of transcription at time t is then given by $-dL(t)/dt$. The mean elongation velocity is determined by a linear fit of $L(t)$ during at least 8 s. A typical measurement is presented in Fig. 2.

Variability

In this subsection we describe the variability observed in the velocity measurements. Fig. 3 shows an example of the variability observed during 1 min for a given enzyme under constant load (5 pN). The velocity is ~40 bp/s for ~20 s (~1 kbp DNA transcribed) and then rises to 80 bp/s for 60 s (~5 kbp DNA transcribed). Fig. 4 shows the observed variability from enzyme to enzyme during a cycle of measurements. In this type of experiment, we alternate loading and relaxation by turning on and off the voltage reference that sets the force: we put the enzyme under load for ~10 s, then relax the load force, then apply a new level of load force for ~10 s, and so on. The values plotted in Fig. 4 arise from linear fits of the data as described above. The difference between the mean velocities measured for different enzymes can be important (compare *open* and *solid circles*). We also noticed that for a given force and a given enzyme, the mean velocity can change during a measurement cycle (see, for example, *open circles* and *crosses* at 5 pN), but it does not depend on the time sequence of the force levels (not shown).

We found that because of 1), the variability for a given enzyme, and 2), the variability from enzyme to enzyme, it was necessary to amass a large amount of data to define the average elongation velocity at a given force and NTP concentration. For example, for the experiments performed with different magnesium ion concentrations (see below, Effect of magnesium), we made sequential measurements on 18 enzymes, allowing 61 linear fits to be performed on transcription records.

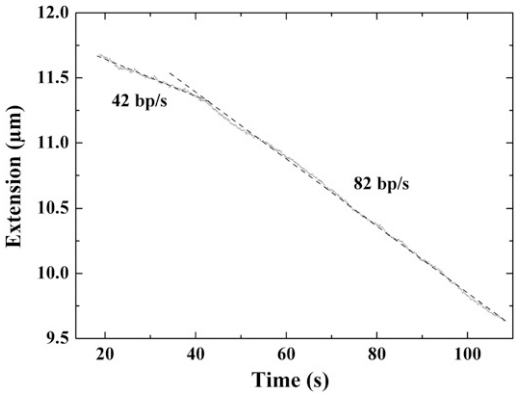

FIGURE 3 Example of experimental recording of extension versus time, with a load force of 5 pN ([NTP] = 150 μM each, $[Mg^{2+}]_{tot} = 8$ mM, $T = 27$°C). This is an example of variability for a given enzyme: at $t \approx 40$ s, the velocity increases from 42 to 82 bp/s. Dotted lines represent linear fits on data.

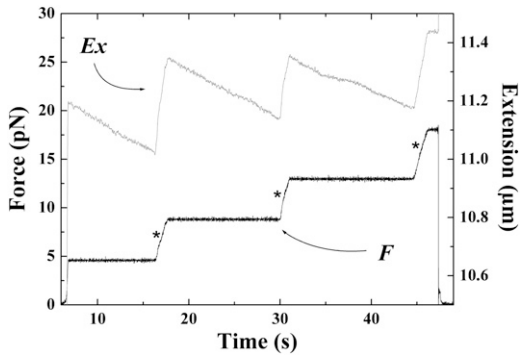

FIGURE 2 Experimental recordings of the applied force (*lower curve*) and of the extension (*upper curve*) versus time, during elongation. Asterisks indicate a change in the voltage reference that imposes the load force. The ''jumps'' in extension curve correspond to the displacement change necessary for the molecule to reach the newly imposed stretching force (to increase the load force, the DNA molecule must be stretched, so that the extension is increased).

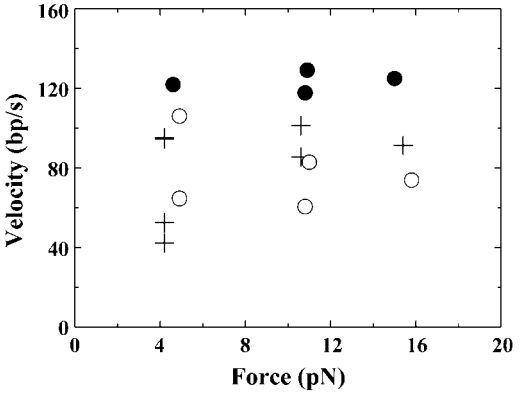

FIGURE 4 Single measurements of elongation velocity versus force. Conditions: [NTP] = 590 μM each; $[Mg^{2+}]_{tot} = 8$ mM; $T = 27$ C°. Each symbol corresponds to a given enzyme and each point corresponds to one measurement (see text); this shows variability 1), for a given enzyme, from ~50 to ~90 bp/s (*crosses*); and 2), from enzyme to enzyme, with mean velocity~130 bp/s (*black circles*) and 60–100 bp/s (*open circles*).

Significant diversity in the elongation rates has also been observed with the *E. coli* RNAP. In single-molecule experiments performed without a load force, the velocities are reported to be quite uniformly distributed about a single mean (25). The authors attributed this diversity to differences in structure. In the case of T7 RNAP under load, we performed the following analysis: for each couple of conditions ([NTP], load force) we normalized the measured velocities by the corresponding average velocity. All the data can then be used to plot a histogram of the measured velocities (Fig. 5). We found that the velocities are quite uniformly distributed around a single mean, as for the *E.coli* RNAP. The standard deviation is ~29% of the mean, which is less than the 42% obtained for the *E. coli* RNAP (25). This difference may arise from the fact that the T7 RNAP is a single-unit enzyme rather than a multisubunit enzyme like the *E. coli* RNAP.

DNA and RNA sequence effects

Among the sequence effects that may be expected are 1), the influence of special sequences known as pause or arrest inducers, and 2), the influence of the different binding constant of the four nucleotides for the active site of the polymerase, an effect we assume here could be correlated to the average (A/T or G/C) content of the DNA template.

Some DNA sequences with a size of ~20 bases (the footprint of the enzyme) and/or RNA sequences that are synthesized during elongation are known to modify the structure of the enzyme and to induce subsequent pauses or arrests (for example, the terminator sequence). This type of effect has been studied, notably, by Davenport et al. (3) with the *E. coli* DNA polymerase in a single-molecule experiment. We did not study such effects with the T7 RNAP, because pauses are extremely rare events with this enzyme. This has been observed both in our experiment using the lambda DNA as a template and in the experiment of Skinner et al. with a T7 DNA template (16).

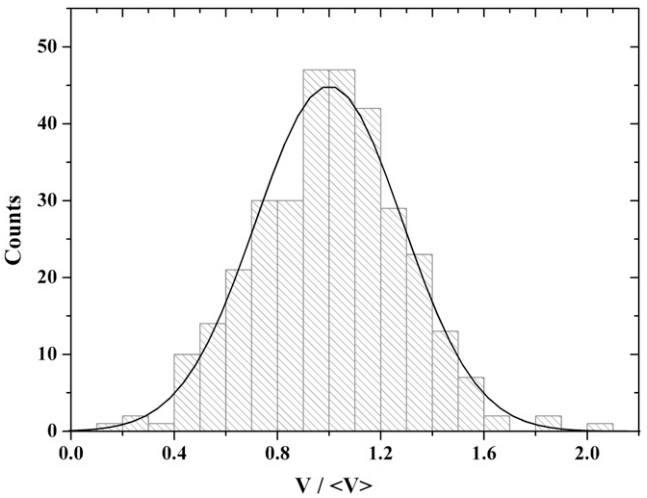

FIGURE 5 Histogram of the normalized velocities ($[Mg^{2+}]_{tot} = 8$ mM). For each couple of conditions ([NTP], load force), each measured elongation velocity is normalized by the mean velocity calculated for this couple of conditions. The curve is a Gaussian fit with the mean imposed as 1 and leads to a standard deviation of 0.285 ($\chi^2 = 4.86$; $r^2 = 0.98$).

If the affinity constant is not the same for the four different nucleotides, the rate of the nucleotide incorporation cycle is expected to be sequence-dependent. K_m values have been measured for the T7 RNAP (26) and a low/high K_m value ratio of ~1:2 was found. To explore even an extreme putative influence of such a nucleotide ''binding effect'', we made a numerical simulation in which we took an overestimated value of 1:10 (instead of 1:2) for the ratio between the transcription velocity for a G or C template base, with respect to an A or T template base. In the Michaelis-Menten kinetic framework, this implies a ratio of K_m(A or T)/K_m(G or C) > 10. For a polymerase transcribing the lambda DNA template, this simulation predicts that significant velocity variations would be observable only over a timescale of <~1 s. Therefore, our data points, which correspond to an average over a long timescale (>8 s), do not allow us to make conclusions about the presence or absence of such a nucleotide ''binding effect'' on the transcription velocity.

The influence of force on velocity

For each of the conditions studied, we only observed velocities distributed about a single mean, i.e., a single mean is defined for each condition. This result clearly does not support two-state models where the enzyme is considered to exist in two different states associated to two different elongation velocities for given conditions of force and nucleotide concentration. The particular experimental trace in Fig. 3 suggests a two-state model; however, this apparent contradiction mainly illustrates that one has to be very careful in drawing a conclusion based on a single measurement.

We measured the velocity of transcription for seven different concentrations of NTP (from 30 μM to 590 μM) and three different levels of force (from 5 to 15 pN). The enzyme is found to be insensitive to force at high nucleotide concentrations, and becomes sensitive to force only at low NTP concentrations (18). This can be seen in Table 2 and Fig. 6, where decrease in velocity is plotted versus [NTP] with the force varied from 5 to 15 pN.

The decrease in mean elongation velocity when increasing the load force from 5 to 15.5 pN is much larger at low NTP concentrations. This suggests that nucleotide binding competes with force. This can also be shown by plotting the data in an LB plot: the data are well fitted by lines that intercept each other at a point on the y axis, indicating that the force acts as a competitive inhibitor (see Table 1). In other words, V_m (~130 bp/s) does not depend on force, and K_m (the reciprocal of the apparent nucleotide binding constant) increases with force.

For molecular motors, two commonly used models are the Brownian ratchet model and the power stroke model. They

TABLE 2 Mean elongation velocity

Force NTP	29 μM	50 μM	73 μM	100 μM	147 μM	235 μM	588 μM
5 pN	25.6 (1.2)	29.5 (1.5)	38.3 (1.5)	46.9 (4.6)	59.6 (3.8)	69.4 (3.4)	98.3 (7.4)
11.5 pN	19.0 (1.4)	25.3 (1.6)	32.1 (1.8)	40.1 (6.9)	50.5 (2.9)	69.4 (3.9)	97.5 (6.7)
15.5 pN	14.4 (1.3)	21.1 (1.9)	28.4 (3.9)	-	48.2 (2.3)	66.8 (4.5)	98.4 (10.5)
dV_{rel}	44%	28%	26%		19%	4%	0%

Mean elongation velocity measured for seven different NTP concentrations and three different load forces ($[Mg^{2+}]_{tot} = 8$ mM). Numbers in parentheses are the standard error of the mean. dV_{rel}, percentage decrease in velocity when force is varied from 5 to 15 pN.

are of opposite nature. In the Brownian ratchet model, thermal fluctuations are assumed to be sufficient to produce movement, provided that a chemical reaction is maintained out of equilibrium (27,28). With this model, the energy dissipated upon nucleotide hydrolysis (in the case of transcription) only induces irreversibility, i.e., polymerization will be biased forward. In the power stroke model, the chemical energy is directly converted into mechanical work. The different crystallographic structures of the enzyme can help to determine which model applies to T7 RNAP. Crystallographic structures of the elongation complex of the T7 RNAP have been obtained with various substrates, yielding three different structures (14). From these structures and the structures obtained with other polymerases (29–31), it appears that the main conformational change occurring during elongation is the rotation of the O helix (a helix that interacts with the pyrophosphate part of the nucleotide), which takes place at each cycle of nucleotide incorporation. The enzyme alternates between a competent ''closed state'' and an incompetent ''open state''. These three states are 1), the closed ''NTP bound'' state (E_{post}-NTP), in which the arrival of a correct NTP has stabilized the enzyme; 2), the closed ''Pretranslocated'' state (E_{pre}-PPi), where catalysis has just occurred but PPi has not yet been released; and the open ''Posttranslocated'' state (E_{post}) just after forward motion along DNA.

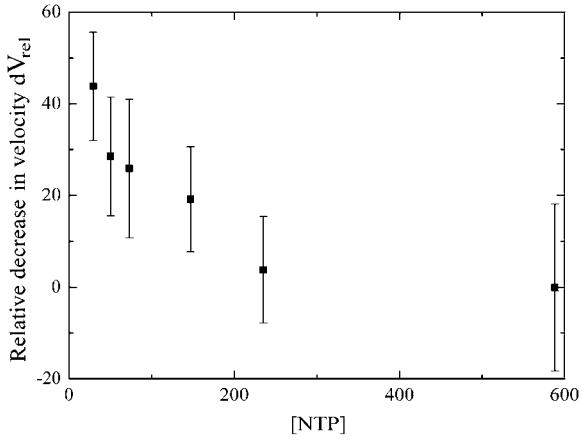

FIGURE 6 Relative decrease in velocity (percentage) is plotted versus NTP concentration, when the load force is varied from 5 to 15 pN. The obtained data show a decreasing function, as expected in a competitive inhibition kinetic.

Yin and Steitz (14) interpret their structural data according to the following scheme:

$$E_{pre}\text{-PPi} \underset{k_-(F)}{\overset{k_+(F)}{\rightleftarrows}} E_{post} \underset{+NTP}{\overset{K_{Dis}}{\rightleftarrows}} E_{post}\text{-NTP} \overset{k_{cat}}{\rightarrow} E_{pre}\text{-PPi},$$

where the motion of the enzyme is power-stroked by the PPi release. In the case of very low [PPi], the forward movement becomes irreversible. In this case, the Michaelis-Menten constants V_m and K_m decrease with increasing force, but the ratio K_m/V_m is independent of force ($1/V_m = 1/k_+(F) + 1/k_{cat}$ and $K_m(F) = K_{Diss} \times k_+(F)/(k_{cat} + k_+(F))$). This corresponds to the uncompetitive inhibition case (Table 1). This model does not match our experimental data ($\chi^2 = 5.5 \times 10^{-6}$ vs. $\chi^2 = 0.6 \times 10^{-6}$ in the case of competitive inhibition).

Our single-molecule experiments, however, suggest instead that a load force acts as a competitive inhibitor. This corresponds to a model where a force opposing forward motion will, in the case of low [PPi], push the enzyme backward from the posttranslocated state, E_{post}, to a pretranslocated state, E^*_{pre}, a pretranslocated complex in the absence of PPi. The E^*_{pre} state can be interpreted in two ways, the corresponding schemes (see below) leading to the same Michaelis-Menten expression of velocity. In the first scheme, E^*_{pre} is an intermediate state between E_{pre}-PPi and E_{post}:

$$E_{pre}\text{-PPi} \underset{k_-}{\overset{k_+}{\rightleftarrows}} E^*_{pre} \overset{K(F)}{\rightleftarrows} E_{post} \underset{+NTP}{\overset{K_{Dis}}{\rightleftarrows}} E_{post}\text{-NTP} \overset{k_{cat}}{\rightarrow} E_{pre}\text{-PPi}.$$

This is the view of Guo and Sousa for T7 RNAP (32) and of Marchand et al. for HIV-1 reverse transcriptase (33).

In the second scheme, E^*_{pre} is seen as a state branching off the main pathway:

$$E_{pre}\text{-PPi} \underset{k_-(F)}{\overset{k_+(F)}{\rightleftarrows}} E_{post} \underset{+NTP}{\overset{K_{Dis}}{\rightleftarrows}} E_{post}\text{-NTP} \overset{k_{cat}}{\rightarrow} E_{pre}\text{-PPi}.$$
$$\qquad\qquad \uparrow\downarrow K(F)$$
$$\qquad\qquad E^*_{pre}$$

In the case of uncompetitive inhibition, the relative decrease in velocity dV_{rel} from a high level of force, F_2, to a lower level of force, F_1, $dV_{rel} = (V_1 - V_2)/V_1$ can be written using the Michaelis-Menten expression of velocity: $dV_{rel} = \gamma \times [NTP]/(1 + \beta \times [NTP])$, where γ and β are positive. dV_{rel} is thus expected to increase with the nucleotide concentration. This can be understood as follows: at low [NTP], on one hand, the limiting step is NTP-binding, and if the force were to act on the PPi release step its action would not be relevant;

on the other hand, at high [NTP], the limiting steps are catalysis and/or PPi release: the action of force is expected to be more relevant.

The experimental results clearly suggest that dV_{rel} decreases when [NTP] is increased (Fig. 6). This is another argument for discarding the uncompetitive inhibition model. The data are more consistent with a competitive inhibition, where dV_{rel} can be written $dV_{rel} = \lambda/(1 + [NTP])$, where λ is positive. dV_{rel} is then expected to decrease when [NTP] rises. In fact, if the force is competing with NTP binding, its effect is indeed expected to be more relevant at low [NTP]. Our experimental data are thus more consistent with a model where the enzyme wobbles between a pre- and a posttranslocated state, i.e., the Brownian ratchet model.

In the presence of very low [PPi], as in our experiment (18), and assuming k_{cat} to be lower than other constants, the two schemes considered before (namely, E^*_{pre} as an intermediate state between $E_{pre\text{-}PPi}$ and E_{post}, or E^*_{pre} as a state branching off the main pathway) actually lead to the same expression for velocity as a function of force, with V_m constant and K_m decreasing with a rising force: $V_m = k_{cat}$ and $K_m(F) = K_{Diss}\ (1 + K(F))$, where K_{diss} is the dissociation constant for NTP. By introducing ΔG_0, the free energy difference between E^*_{pre} and E_{post}, and using $d = 0.34$ nm as the step size, one gets $K_m(F) = K_{diss}(1 + \exp[\Delta G_0/kT]\exp[Fd/kT])$. Fitting K_{diss} and ΔG_0 to the experimental data (18) yields $K_{diss} = 124\ \mu$M and $\Delta G_0 = -1.3\ kT$. From our single-molecule data, we estimated (18) the energy change between E^*_{pre} and E_{post} to be $-1.3\ kT$, i.e., -0.8 kcal/mol. Yin and Steitz (14) estimate that the open posttranslocation conformation (E_{post}) is ~3 kcal/mol more stable than E^*_{pre}. However, in that case, the system considered does not include changes in the transcription bubble. Therefore, if we take into account the free energy necessary to balance the broken DNA-RNA basepair that occurs during forward motion (which we estimate to be on average of the order of $3\ kT = 1.8$ kcal/mol (18)), the difference between E^*_{pre} and E_{post} complexed with the DNA template and nascent RNA is thus estimated as follows: -3 kcal/mol + 1.8 kcal/mol = -1.2 kcal/mol, an estimation viewed as compatible with the value of -0.8 kcal/mol deduced from our single-molecule experiments.

It is now worth stressing that an energy change of $1\ kT$ (associated with a thermal fluctuation, or with a forward bias) occurring with a translocation over a distance of 0.34 nm (the step size of 1 bp in the nucleotide addition cycle) may be formally associated with a force $F = \Delta E/\text{step size} \sim 12$ pN: in other words, an energy of $1\ kT$ is sufficient to produce work against a force of the order of ~10 pN applied on an interbase distance. Let us take also a different perspective: for the T7 RNAP, the stall force appears to be in the range 20–25 pN as typically observed with our experiments, giving a maximum work of ~8 pN.nm $\approx 2\ kT$. This is another way to argue that the forward motion of the T7 RNAP is not associated with a large energy change. However, this argument is to be taken with some caution, as it is assumed that the enzyme force limitation does not occur because of a deformation (or a partial denaturation) of the enzyme itself.

Effect of magnesium

To further analyze the T7 RNAP enzyme, we studied the influence of the magnesium ion concentration on the elongation mode of the enzyme. Magnesium is a cofactor of the nucleic acid polymerization catalyzed by DNA and RNA polymerases. The positions of two magnesium ions are conserved in the active site of all presently crystallized polymerases and it has been proposed that these two ions are essential for catalysis. A corresponding model has been proposed for DNA polymerases (34) and can be easily applied to RNA polymerases, since the most important domains and the amino acids involved in the active site are conserved among these enzymes (at least among Pol I family). We were interested in studying how magnesium could modify the transcription velocity and how this effect might depend on force. The rationale of our studies was that by varying the magnesium ion concentration it should be possible to perturb the kinetics in the particular step within the catalytic cycle where catalysis occurs.

In the following, [NTP] stands for the (equal) concentration of each type of nucleotide introduced in the sample, and $[NTP]_{tot}$ stands for the total nucleotide concentration introduced, i.e., $4 \times [NTP]$. In solution, one magnesium ion, Mg^{2+}, can react with one nucleotide, NTP^{4-}, to form $MgNTP^{2-}$ with a dissociation constant, K_d, of ~30 μM at 37°C. A second magnesium ion can react with the $MgNTP^{2-}$ complex, but with a much larger K_d of ~25 mM. The other species have either a large K_d or are minority species in our buffer (see Storer and Cornishbowden (35) for studies of reactions between ATP and other species). We therefore assume that in the transcription mix, due to the low K_d, essentially each nucleotide reacts with one magnesium ion to form $MgNTP^{2-}$ complexes, provided that $[Mg^{2+}]_{tot} > [NTP]_{tot}$ (this is illustrated in Fig. 7). We then assume that one of the two ions in the catalytic site is brought in by the incoming NTP, and the second ion is provided from the pool of free magnesium ions left in solution. This suggests that if $[Mg^{2+}]_{tot} < [NTP]_{tot}$, the free magnesium concentration ($[Mg^{2+}]_{free}$) will be very low; in such conditions, the elongation velocity is expected to be drastically reduced, a scenario that has been observed with HIV-1 reverse transcriptase, which is closely related to T7 RNAP (36).

To study the influence of magnesium, we performed experiments with high $[NTP]_{tot}$ to avoid limiting the NTP binding step, and we varied $[Mg^{2+}]_{tot}$. We performed experiments using five different conditions: $\{[Mg^{2+}]_{tot}, [NTP]_{tot}\} = \{28\text{ mM}, 15.2\text{ mM}\}$, $\{22\text{ mM}, 7.2\text{ mM}\}$, $\{15\text{ mM}, 15.2\text{ mM}\}$, $\{8.5\text{ mM}, 6.8\text{ mM}\}$, and $\{8\text{ mM}, 15.6\text{ mM}\}$. By compiling all the data, we observed that given a level of force,

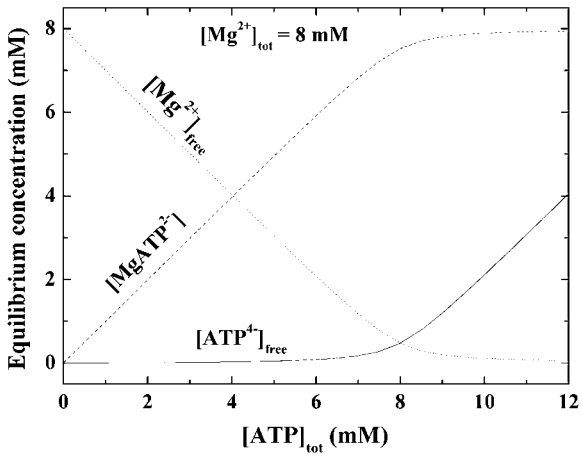

FIGURE 7 Equilibrium concentrations of $[Mg^{2+}]_{free}$, $[MgATP^{2-}]$, and $[ATP^{4-}]_{free}$ versus $[ATP^{4-}]_{tot}$ expected for a dissociation constant, K_D, of 30 μM between ATP^{4-} and Mg^{2+}, with the total concentration of magnesium ($[Mg^{2+}]_{tot}$) fixed at 8 mM (the concentration used in Thomen et al. (18)). It shows that almost all ATP^{4-} molecules react with one magnesium ion as long as $[ATP^{4-}]_{tot} < [Mg^{2+}]_{tot}$.

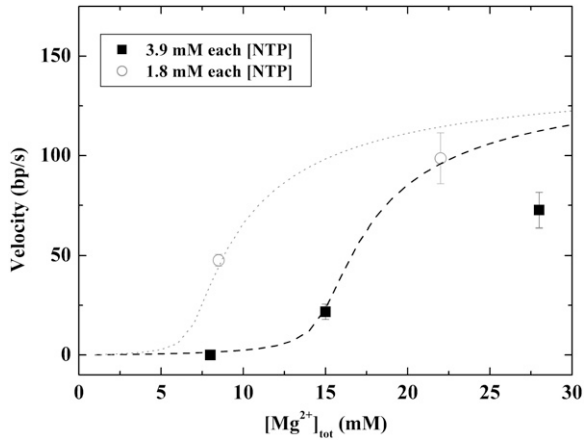

FIGURE 8 Mean elongation velocity versus $[Mg^{2+}]_{tot}$ at fixed $[NTP^{4-}]_{tot}$. No transcription activity was observed in experiments performed at $\{[Mg^{2+}]_{tot} = 8$ mM, $[NTP^{4-}]_{tot} = 15.6$ mM$\}$, the translocation being apparently inhibited. $[Mg^{2+}]_{tot}$ and $[NTP^{4-}]_{tot}$ are the total concentrations of magnesium and NTP, respectively, introduced in solution. The dotted line is the plot of Eq. 1 using the values of K and K_{NTP} determined in Thomen et al. (18), and the value of K_{Mg} and k_{cat} determined in this work (see text).

1. For a given $[NTP]_{tot}$, a rising $[Mg^{2+}]_{tot}$ increases the mean elongation velocity. (Fig. 8)
2. For a given $[Mg^{2+}]_{tot}$, the mean elongation velocity first increases when $[NTP]_{tot}$ increases ($MgNTP^{2-}$ is limiting), then decreases when $[Mg^{2+}]_{free}$ becomes limiting. (Fig. 9)
3. No transcription activity is observed when $[NTP]_{tot} \approx 2 \times [Mg^{2+}]_{tot}$ (Figs. 8 and 9).

These features are consistent with the above remarks on the interactions between NTP and magnesium ions. This leads us to propose a modified scheme for elongation, which takes into account the magnesium ions. The simplest scheme is as follows:

$$E_{pre} \overset{K}{\rightleftarrows} E_{post} \underset{+MgNTP^{2-}}{\overset{K_{NTP}}{\rightleftarrows}} E_{post}\text{-}(MgNTP^{2-}) \underset{+Mg^{2+}}{\overset{K_{Mg}}{\rightleftarrows}} Mg^{2+} E_{post}(MgNTP^{2-}) \overset{k_{cat}}{\rightarrow} E_{post} + PPi + 2Mg^{2+}.$$

A second magnesium ion is assumed to bind to the polymerase once the incoming nucleotide (already complexed with a first magnesium ion) has bound, because the interaction between the metallic ions and the polymerase is expected to be promoted by the triphosphate part of the nucleotide. In the model of rapid equilibrium, the catalytic constant k_{cat} is considered negligible compared to other constants, and such a scheme allows a Michaelis-Menten expression of the velocity, V:

$$\frac{1}{V} = \frac{1}{k_{cat}}\left(1 + 4(1+K)\frac{K_{Mg}K_{NTP}}{[MgNTP^{2-}][Mg^{2+}]_{free}} + \frac{K_{Mg}}{[Mg^{2+}]_{free}}\right).$$

The constant K (described in the latter subsection) corresponds to the equilibrium $E_{pre} - E_{post}$. K_{NTP} is the dissociation constant for $MgNTP^{2-}$. The factor 4 occurs because one-fourth of all nucleotides (the correct type to be incorporated for a given template base) is able to bind the active site at each step of nucleotide addition, whereas all types of nucleotides bind magnesium. [NTP] was always much higher than K_{NTP}, so that $K_{NTP} \ll [MgNTP^{2-}]$. The above expression simplifies then to

$$V \approx \frac{k_{cat}}{1 + K_{Mg}/[Mg^{2+}]_{free}}.$$

It is possible to estimate K_{Mg} and k_{cat} in our experiment by plotting $1/\langle V\rangle$ against $1/[Mg^{2+}]_{free}$ (see Fig. 10): a linear dependence appears compatible with the data, and we estimated that $K_{Mg} \approx 3.2$ mM and $k_{cat} \approx 141$ bp/s by fitting the experimental data. The K_{Mg} value is consistent with the bulk measurements of Young et al. (37) (2.1 $\pm$ 1.6 mM) and Woody et al. (38) ($\sim$2 mM). One notes that this value is lower than the dissociation constant between $MgNTP^{2-}$ and Mg^{2+} (25 mM), consistent with the initial hypothesis that the Mg^{2+} ions free in solution are available for the polymerase.

Using the estimated parameters K_{Mg} and k_{cat} obtained in the latter fit, and the values of K_{NTP} and K deduced earlier

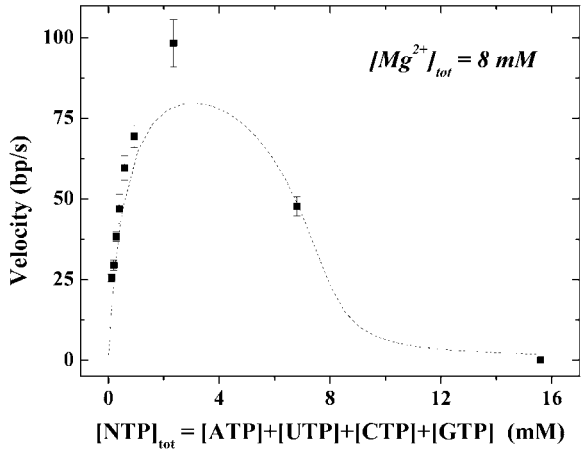

FIGURE 9 Mean elongation velocity versus $[NTP^{4-}]_{tot}$ at fixed $[Mg^{2+}]_{tot}$. No transcription activity was observed in experiments performed at $\{[Mg^{2+}]_{tot} = 8$ mM, 3.9 mM of each type of NTP, i.e., $[NTP^{4-}]_{tot} = 15.6$ mM$\}$, the translocation being apparently inhibited. The seven first points correspond to measurements from a previous study (18). $[Mg^{2+}]_{tot}$ and $[NTP^{4-}]_{tot}$ stand for the total concentrations of magnesium and NTP, respectively, introduced in the solution. The dotted line is the plot of Eq. 1 using the values of K and K_{NTP} determined in Thomen et al. (18) and the values of K_{Mg} and k_{cat} determined in this work (see text).

(18), using Eq. 1 we plot the expected curves that relate velocity to $[NTP]_{tot}$ (Fig. 9) and velocity to $[Mg^{2+}]_{tot}$ (Fig. 8). The model qualitatively fits the data.

What is the influence of force on the elongation velocity when $[Mg^{2+}]_{free}$ is a limiting factor? In our measurements, the mean elongation velocity decreased when $[Mg^{2+}]_{free}$ was limiting, but we did not observe an influence of the force on the average velocity (Figs. 10 and 11). In the following

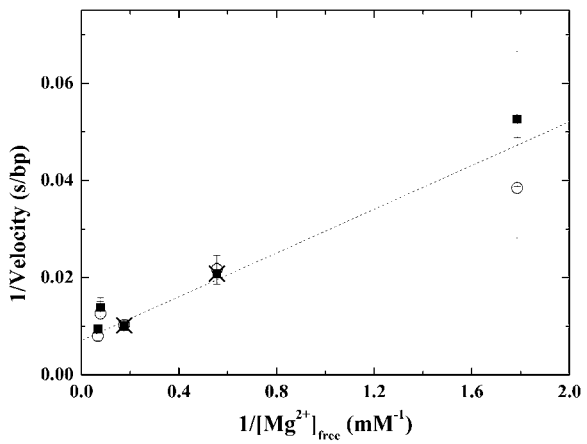

FIGURE 10 Inverse of the mean elongation velocity versus the inverse of $[Mg^{2+}]_{free}$, for different levels of force. In all cases, the NTP concentration was not limiting (>600 μM each); thus, the decrease in velocity is mainly due to limiting $[Mg^{2+}]_{free}$. The dotted line is a linear fit of the data, giving an estimate of $K_{Mg} \approx 3.2$ mM. $[Mg^{2+}]_{free}$ stands for free magnesium ions and is calculated using $[Mg^{2+}]_{tot}$ and $[NTP^{4-}]_{tot}$ and assuming a dissociation constant of $K_D = 30$ μM for the reaction $ATP^{4-} + Mg^{2+} \leftrightarrow MgATP^{2-}$. Squares, $F \approx 5$ pN; open circles, $F \approx 11.5$ pN; crosses, $F \approx 15.5$ pN.

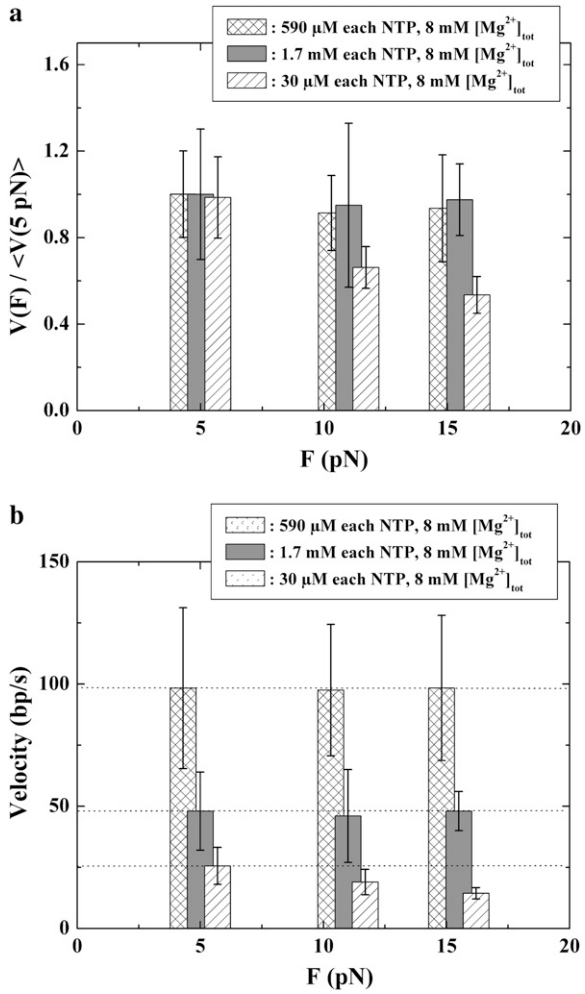

FIGURE 11 (*a*) Comparison of mean elongation velocities relative to the mean value measured at 5 pN, for three different conditions: 1), [NTP] and $[Mg^{2+}]_{free}$ are not limiting (*cross-hatched bars*); 2), $[Mg^{2+}]_{free}$ is limiting, but not [NTP] (*gray bars*); 3), [NTP] is limiting, but not $[Mg^{2+}]_{free}$ (*hatched bars*). (*b*) The same type of plot, but with absolute velocities. One can see that in the case where $[Mg^{2+}]_{free}$ is limiting, but not [NTP], the velocity is decreased, but no effect of force is observed. The histograms show that the elongation velocity is dependent on force only when [NTP] is limiting.

condition, [NTP] = 1.7 mM (each NTP type), and $[Mg^{2+}]_{tot} =$ 8 mM, it is expected that $[Mg^{2+}]_{free} \approx 1.3$ mM and $[MgNTP^{2-}] \approx 6.7$ mM (see Fig. 7). $[Mg^{2+}]_{free}$ is therefore below the K_{Mg} ($\sim$3.2 mM) and is expected to be limiting.

One can thus conclude that low $[Mg^{2+}]_{free}$ limits a step in the catalytic cycle, which is not sensitive to force. Assuming that the load force acts essentially on the translocation step, this implies that the magnesium ion limitation acts on a step that is not coupled to forward motion. If one refers to the two-ion catalysis model proposed by Brautigam and Steitz (34), one can infer that magnesium ions are involved in a step concomitant with hydrolysis. Our measurements suggest therefore that the hydrolysis step is not coupled with forward motion. This agrees with our previous interpretation deduced from LB plots (previous section), that forward motion takes

place in a step concomitant to nucleotide binding, and does not occur upon NTP cleavage.

CONCLUSION

In this study, we investigated the transcription mechanism of the T7 RNAP in a single-molecule experimental setup. Our measurements of the elongation velocity show that variability is important both for a given molecule and from molecule to molecule. This underlines that a lot of data must be accumulated to draw a compelling conclusion from single-molecule experiments. The distribution of velocity was found to be unimodal, excluding a two-state model, and consistent with previous results obtained with *E. coli* RNAP. The T7 RNAP is composed of a single unit, and is quite processive, making this enzyme a good model for the study of transcription elongation.

This work also illustrates how one can make use of the response of a molecular motor to variations in both load force and the concentration of a cofactor. A general way to identify the different steps of a complex reaction cycle is to explore the parameter space to find the conditions that make a particular step globally rate-limiting. In the example described here, this was achieved by imposing a load force to limit the step of forward motion and by decreasing the substrate concentration, [NTP], to limit the substrate binding step. By decreasing the cofactor concentration (here, $[Mg^{2+}]_{free}$), the steps affected by the cofactor can be revealed, and by applying an external mechanical force it can be determined whether these steps are related, or not, to the movement of the motor along the DNA.

By measuring the elongation velocity under mechanical load, we were able to conclude that force acts as a competitive inhibitor, with V_m constant and K_m decreasing when the load force is increased, results that are consistent with a Brownian Ratchet model. The measurements performed at different magnesium ion concentrations and saturating NTP concentration confirmed that free magnesium ion concentration may become a limiting factor of transcription, and showed that the enzyme is insensitive to force at low concentrations of free magnesium ions. This demonstrates that the magnesium ion, a cofactor of transcription, is involved in a step that is not related to the forward motion. This is in full agreement with the two-metal-ions model of catalysis proposed earlier (34), arguing that magnesium ions are involved in the hydrolysis step.

REFERENCES

1. Erie, D. A., T. D. Yager, and P. H. Vonhippel. 1992. The single-nucleotide addition cycle in transcription: a biophysical and biochemical perspective. *Annu. Rev. Biophys. Biomol. Struct.* 21:379–415.
2. Alberts, B., A. Johnson, J. Lewis, M. Raff, K. Roberts, and P. Walter. 2002. Molecular Biology of the Cell, 4th ed. Garland, New York.
3. Davenport, R. J., G. J. L. Wuite, R. Landick, and C. Bustamante. 2000. Single-molecule study of transcriptional pausing and arrest by E-coli RNA polymerase. *Science.* 287:2497–2500.
4. Wuite, G. J. L., S. B. Smith, M. Young, D. Keller, and C. Bustamante. 2000. Single-molecule studies of the effect of template tension on T7 DNA polymerase activity. *Nature.* 404:103–106.
5. Smith, D. E., S. J. Tans, S. B. Smith, S. Grimes, D. L. Anderson, and C. Bustamante. 2001. The bacteriophage $\phi 29$ portal motor can package DNA against a large internal force. *Nature.* 413:748–752.
6. Visscher, K., M. J. Schnitzer, and S. M. Block. 1999. Single kinesin molecules studied with a molecular force clamp. *Nature.* 400:184–189.
7. Schnitzer, M. J., K. Visscher, and S. M. Block. 2000. Force production by single kinesin motors. *Nat. Cell Biol.* 2:718–723.
8. Wang, M. D., M. J. Schnitzer, H. Yin, R. Landick, J. Gelles, and S. M. Block. 1998. Force and velocity measured for single molecules of RNA polymerase. *Science.* 282:902–907.
9. Adelman, K., A. La Porta, T. J. Santangelo, J. T. Lis, J. W. Roberts, and M. D. Wang. 2002. Single molecule analysis of RNA polymerase elongation reveals uniform kinetic behavior. *Proc. Natl. Acad. Sci. USA.* 99:13538–13543.
10. Maier, B., D. Bensimon, and V. Croquette. 2000. Replication by a single DNA polymerase of a stretched single-stranded DNA. *Proc. Natl. Acad. Sci. USA.* 97:12002–12007.
11. Neuman, K. C., E. A. Abbondanzieri, R. Landick, J. Gelles, and S. M. Block. 2003. Ubiquitous transcriptional pausing is independent of RNA polymerase backtracking. *Cell.* 115:437–447.
12. Itoh, H., A. Takahashi, K. Adachi, H. Noji, R. Yasuda, M. Yoshida, and K. Kinosita. 2004. Mechanically driven ATP synthesis by F-1-ATPase. *Nature.* 427:465–468.
13. Abbondanzieri, E. A., W. J. Greenleaf, J. W. Shaevitz, R. Landick, and S. M. Block. 2005. Direct observation of base-pair stepping by RNA polymerase. *Nature.* 438:460–465.
14. Yin, Y. W., and T. A. Steitz. 2004. The structural mechanism of translocation and helicase activity in T7 RNA polymerase. *Cell.* 116:393–404.
15. Temiakov, D., V. Patlan, M. Anikin, W. T. McAllister, S. Yokoyama, and D. G. Vassylyev. 2004. Structural basis for substrate selection by T7 RNA polymerase. *Cell.* 116:381–391.
16. Skinner, G. M., C. G. Baumann, D. M. Quinn, J. E. Molloy, and J. G. Hoggett. 2004. Promoter binding, initiation, and elongation by bacteriophage T7 RNA polymerase: a single-molecule view of the transcription cycle. *J. Biol. Chem.* 279:3239–3244.
17. Yin, H., M. D. Wang, K. Svoboda, R. Landick, S. M. Block, and J. Gelles. 1995. Transcription against an applied force. *Science.* 270: 1653–1657.
18. Thomen, P., P. J. Lopez, and F. Heslot. 2005. Unravelling the mechanism of RNA-polymerase forward motion by using mechanical force. *Phys. Rev. Lett.* 94:128102.
19. Yin, Y. W., and A. A. Steitz. 2002. Structural basis for the transition from initiation to elongation transcription in T7 RNA polymerase. *Science.* 298:1387–1395.
20. Tahirov, T. H., D. Temiakov, M. Anikin, V. Patlan, W. T. McAllister, D. G. Vassylyev, and S. Yokoyama. 2002. Structure of a T7 RNA polymerase elongation complex at 2.9 Å resolution. *Nature.* 420: 43–50.
21. Bockelmann, U., P. Thomen, B. Essevaz-Roulet, V. Viasnoff, and F. Heslot. 2002. Unzipping DNA with optical tweezers: high sequence sensitivity and force flips. *Biophys. J.* 82:1537–1553.
22. Maslak, M., and C. T. Martin. 1994. Effects of solution conditions on the steady-state kinetics of initiation of transcription by T7 RNA polymerase. *Biochemistry.* 33:6918–6924.
23. Brieba, L. G., V. Gopal, and R. Sousa. 2001. Scanning mutagenesis reveals roles for helix N of the bacteriophage T7 RNA polymerase thumb subdomain in transcription complex stability, pausing, and termination. *J. Biol. Chem.* 276:10306–10313.

24. Odijk, T. 1995. Stiff chains and filaments under tension. *Macromolecules*. 28:7016–7018.

25. Tolic-Norrelykke, S. F., A. M. Engh, R. Landick, and J. Gelles. 2004. Diversity in the rates of transcript elongation by single RNA polymerase molecules. *J. Biol. Chem.* 279:3292–3299.

26. Arnold, S., M. Siemann, K. Scharnweber, M. Werner, S. Baumann, and M. Reuss. 2001. Kinetic modeling and simulation of in vitro transcription by phage T7 RNA polymerase. *Biotechnol. Bioeng.* 72: 548–561.

27. Parrondo, J. M. R., and B. J. De Cisneros. 2002. Energetics of Brownian motors: a review. *Appl. Phys. A.* 75:179–191.

28. Astumian, R. D. 1997. Thermodynamics and kinetics of a Brownian motor. *Science*. 276:917–922.

29. Li, Y., S. Korolev, and G. Waksman. 1998. Crystal structures of open and closed forms of binary and ternary complexes of the large fragment of *Thermus aquaticus* DNA polymerase I: structural basis for nucleotide incorporation. *EMBO J.* 17:7514–7525.

30. Doublie, S., S. Tabor, A. M. Long, C. C. Richardson, and T. Ellenberger. 1998. Crystal structure of a bacteriophage T7 DNA replication complex at 2.2 Åresolution. *Nature*. 391:251–258.

31. Huang, H. F., R. Chopra, G. L. Verdine, and S. C. Harrison. 1998. Structure of a covalently trapped catalytic complex of HIV-I reverse transcriptase: implications for drug resistance. *Science.* 282:1669–1675.

32. Guo, Q., and R. Sousa. 2006. Translocation by T7 RNA polymerase: a sensitively Brownian ratchet. *J. Mol. Biol.* 358:241–254.

33. Marchand, B., E. P. Tchesnokov, and M. Gotte. 2007. The pyrophosphate analogue foscarnet traps the pre-translocational state of HIV-1 reverse transcriptase in a Brownian ratchet model of polymerase translocation. *J. Biol. Chem.* 282:3337–3346.

34. Brautigam, C. A., and T. A. Steitz. 1998. Structural and functional insights provided by crystal structures of DNA polymerases and their substrate complexes. *Curr. Opin. Struct. Biol.* 8:54–63.

35. Storer, A. C., and A. Cornishbowden. 1976. Concentration of $MgATP^{2-}$ and other ions in solution: calculation of true concentrations of species present in mixtures of associating ions. *Biochem. J.* 159:1–5.

36. Goldschmidt, V., J. Didierjean, B. Ehresmann, C. Ehresmann, C. Isel, and R. Marquet. 2006. Mg^{2+} dependency of HIV-1 reverse transcription, inhibition by nucleoside analogues and resistance. *Nucleic Acids Res.* 34:42–52.

37. Young, J. S., W. F. Ramirez, and R. H. Davis. 1997. Modeling and optimization of a batch process for in vitro RNA production. *Biotechnol. Bioeng.* 56:210–220.

38. Woody, A. Y. M., S. S. Eaton, P. A. Osumi-Davis, and R. W. Woody. 1996. Asp537 and Asp812 in bacteriophage T7 RNA polymerase as metal ion-binding sites studied by EPR, flow-dialysis, and transcription. *Biochemistry.* 35:144–152.